Available online at www.sciencedirect.com
SCIENCE DIRECT
Biochemical and Biophysical Research Communications 346 (2006) 89–94
BBRC
www.elsevier.com/locate/ybbrc

Acetylcholinesterase triggers the aggregation of PrP 106–126 ☆

M. Pera [a], S. Román [a], M. Ratia [a], P. Camps [c], D. Muñoz-Torrero [c], L. Colombo [b], C. Manzoni [b], M. Salmona [b], A. Badia [a], M.V. Clos [a,*]

[a] *Departament de Farmacologia, de Terapèutica i de Toxicología, Institut Neurociències, Universitat Autónoma de Barcelona, Barcelona, Spain*
[b] *Department of Molecular Biochemistry and Pharmacology, Istituto di Ricerche Farmacologiche "Mario Negri", Milan, Italy*
[c] *Laboratori de Química Farmacéutica (Unitat Associada al CSIC), Facultat de Farmàcia, Universitat de Barcelona, Barcelona, Spain*

Received 24 April 2006
Available online 24 May 2006

Abstract

Acetylcholinesterase (AChE), a senile plaque component, promotes amyloid-β-protein (Aβ) fibril formation in vitro. The presence of prion protein (PrP) in Alzheimer's disease (AD) senile plaques prompted us to assess if AChE could trigger the PrP peptides aggregation as well. Consequently, the efficacy of AChE on the PrP peptide spanning-residues 106–126 aggregation containing a coumarin fluorescence probe (coumarin-PrP 106–126) was studied. Kinetics of coumarin-PrP 106–126 aggregation showed a significant increase of maximum size of aggregates (MSA), which was dependent on AChE concentration. AChE-PrP 106–126 aggregates showed the tinctorial and optical amyloid properties as determined by polarized light and electronic microscopy analysis. A remarkable inhibition of MSA was obtained with propidium iodide, suggesting that AChE triggers PrP 106–126 and Aβ aggregation through a similar mechanism. Huprines (AChE inhibitors) also significantly decreased MSA induced by AChE as well, unveiling the potential interest for some AChE inhibitors as a novel class of potential anti-prion drugs.

Keywords: Acetylcholinesterase; Acetylcholinesterase inhibitors; Huprines; Amyloid aggregation process; Amyloid-β-protein; Alzheimer's disease; Prion protein; PrP 106–126

Transmissible spongiform encephalopathies are caused by an extra-cellular surface protein, the scrapie prion protein (PrP^{Sc}), which is an aberrant form of normal and functional cellular prion protein (PrP^{C}). The pathological hallmarks of these diseases are the accumulation and deposition of PrP^{Sc} in the form of amyloid fibrils in the central nervous system [1]. The transition from PrP^{C} to PrP^{Sc} involves conformational changes with a decrease in the α-helical and an increase in the β-sheet secondary-structure content [2]. This conversion reaction induces remarkable changes in the physicochemical properties of the protein, including insolubility in non-denaturating detergents and partial resistance to proteinase K digestion [3].

In some Alzheimer's disease (AD) patients, amyloid-β-peptide (Aβ) and prion pathologies coexist [4,5]. Actually, a common spatial pattern of protein deposition in both pathologies has also been described [6], and the nature, size, and morphology of multicentric PrP^{Sc} plaques are similar to Aβ-immunoreactive senile plaques [7]. In addition, Aβ-positive senile plaques in AD brains commonly contain PrP deposits [5], while sporadically Aβ-positive senile plaques have also been identified in prion diseases such as Creutzfeldt–Jakob disease (CJD) and Gerstmann–Sträussler–Scheinker disease (GSS) [4,8]. The interrelations between the cholinergic system and PrP^{C} were suggested owing to the location of prion protein at the neuromuscular junction [9] and the co-immunoprecipitation with the β-4 subunit nicotinic receptor in the normal

☆ *Abbreviations:* AChE, acetylcholinesterase; Aβ, amyloid-β-protein; AD, Alzheimer's disease; PrP, prion protein; MSA, maximum size of aggregates; PrP^{C}, cellular prion protein; PrP^{Sc}, disease specific prion protein; CJD, Creutzfeldt–Jakob disease; GSS, Gerstmann–Sträussler–Scheinker disease.

* Corresponding author. Fax: +34 935812986.
E-mail address: Victoria.Clos@uab.es (M.V. Clos).

0006-291X/$ - see front matter © 2006 Elsevier Inc. All rights reserved.
doi:10.1016/j.bbrc.2006.04.187

human brain [10]. In addition, an implication of prion proteins in the regulation of the acetylcholine receptor number at the neuromuscular junction and in the central nervous system has also been proposed [11].

Although the mechanism underlying amyloid protein aggregation still remains obscure, it has been demonstrated that acetylcholinesterase (AChE), an important component of cholinergic synapses, co-localizes with Aβ deposits in AD brains and accelerates assembly of amyloid-β peptides [12]. This non-catalytic function of the enzyme has been related to the peripheral anionic site close to the entrance of the active site gorge and it has been widely described that AChE directly promotes the aggregation of Aβ peptide into amyloid fibrils through this peripheral site [12–14]. Moreover, this amyloidogenic effect of AChE is inhibited by propidium iodide, a purely non-specific cholinesterase inhibitor (AChEI) [15], which binds to the peripheral site decreasing Aβ peptide aggregation, and a similar effect can be observed with the non-selective bisquaternary inhibitor, decamethonium [16]. On the contrary, active-site competitive inhibitors, such as edrophonium, did not show any inhibitory effect on Aβ aggregation [16].

In light of these observations, we explored the capacity of AChE to trigger the aggregation of a peptide comprising residues 106–126 of prion protein (PrP 106–126), which corresponds to a segment considered central to both the process of conversion reaction and the pathogenic properties of abnormal PrP isoforms. In fact, this peptide showed high propensity to adopt stable β-sheet secondary structure and to assemble into straight, unbranched amyloid fibrils, ultrastructurally similar to those observed in GSS patients [17–19]. It also induced apoptotic death in primary cultures of hippocampal [20], cortical [21], and cerebral neurons [22], and exerted a trophic action on glial cells [23]. The data reported in this paper indicate that similar to Aβ, PrP 106–126 aggregation is triggered by AChE through an identical mechanism.

Materials and methods

Peptide synthesis. The peptide corresponding to the 106–126 segment (KTNMKHMAGAAAAGAVVGGLG) of the human prion protein and a scrambled sequence thereof (NGAKALMGGHGATKVMVGAAA) were synthesized using solid-phase chemistry with a 433A instrument (Applied Biosystems). Fmoc (9-fluorenylmethoxycarbonyl) was used as the protective group for amine residues, and 1-hydroxybenzotriazole and *N*,*N*-dicyclohexylcarbodiimide as activators of carboxylic residues.

Fluorescent peptides were synthesized using Fmoc-K(methoxycoumarin)-OH and a single coumarin moiety was introduced into K106 and K109 residues in the wild type and scrambled sequences, respectively. Peptides were purified by HPLC as previously described [19]; their purity being always above 99.5%.

Time course of AChE-induced PrP 106–126 aggregation. Lyophilized aliquots of the PrP 106–126 peptide and its scrambled analogue, and coumarin-PrP 106–126 and its scrambled analogues were suspended in 100 mM Tris–HCl, pH 7.0, at a concentration of 1 mM. For the formation of amyloid fibrils samples were vigorously mixed and incubated for different interval of times (0, 1, 5, 24, and 72 h) at room temperature and centrifuged at 13,000*g* for 10 min to separate the aggregates from soluble peptide [17]. To evaluate the effectiveness of bovine AChE (Sigma–Aldrich) to trigger PrP 106–126 aggregation to a greater extent co-incubation experiments were carried out with different final concentrations of AChE, ranging from 0.31 to 2.5 μM, and incubated for 48 h at room temperature. At the end of the incubation, samples were immediately deep-frozen and stored at −20 °C until analysis.

To evaluate the effect of AChE on aggregation of coumarin-PrP 106–126 and its scrambled analogue, peptide pellets were washed several times with 100 mM Tris–HCl, pH 7.0, suspended in 10 μL of the same buffer, placed on gelatin-coated slides, and analyzed by fluorescence microscopy (Olympus BXJ1; DAPI filter). Three images of each replicate were selected (at least four experiments run in triplicate) and the maximum size of aggregates (MSA, μm^2) of each image was determined using a standard-image analysis program (Leica Qwin). This value was used to quantify the effects of enzyme and its inhibitors on the aggregation process of PrP 106–126. In no case was the presence of fluorescent aggregates observed in the scrambled coumarin-PrP 106–126 samples in both in the presence or absence of AChE.

Inhibition of AChE-induced PrP 106–126 aggregation by AChE inhibitors. PrP 106–126 or coumarin-PrP 106–126 were incubated in 100 mM Tris–HCl, pH 7.0, for 48 h at room temperature at a final concentration of 1 mM in the presence of different concentrations of non-specific and specific AChE inhibitors, such as propidium iodide concentrations (0.01–100 μM), and huperzine A and tacrine (100 μM) (Sigma–Aldrich), respectively. Huprine X, huprine Y, huprine Z (100 μM) (Laboratori de Química Farmacèutica, Facultat de Farmàcia, Universitat de Barcelona, Barcelona, Spain) a new group of AChE inhibitors obtained by hybridation of huperzine A and tacrine were also evaluated. Parallel control samples devoid of inhibitors or in the presence of inhibitors without AChE were always run. After incubation for 48 h at room temperature, samples were immediately deep-frozen and stored at −20 °C until analysis.

Light and electron microscopy. Peptide pellets were washed several times with 100 mM Tris–HCl, pH 7.0, suspended in 10 μL of the same buffer. Samples were air-dried on gelatin-coated slides, stained with 0.2% Congo Red in 80% ethanol saturated with NaCl, and viewed under polarized light (Leitz DM RB, Oberkochen, Germany). For ultrastructural examination, 5 μL of suspension was applied to Formvar-carbon 200-mesh nickel grids for 2 min, negatively stained with 2% (w/v) uranyl acetate, and observed in an electron microscope (Hitachi H-7000, Hitachi Ltd, Tokyo, Japan).

Statistical analysis. Results are expressed as means ± SEM of MSA of at least four experiments run in triplicate. Variances of groups were compared using one-way ANOVA followed by Dunnett's test for multiple comparisons when appropriate. Differences were established at $p < 0.05$.

Results and discussion

It has been described that Aβ-positive senile plaques in AD brains commonly contain PrP deposits [4,5], and Aβ- and PrP-positive senile plaques in prion diseases such as CJD and GSS disease have been detected [4,8]. AChE, an important component of cholinergic synapses, co-localizes with Aβ deposits in AD brains and directly promotes the aggregation of Aβ-protein into amyloid fibrils through the peripheral anionic site [12–14]. This effect is blocked by propidium iodide, a selective ligand for the peripheral site of AChE [15]. On the other hand, the synthetic PrP 106–126 peptide that shares some chemicophysical and biological properties with human PrP [17,18,20] adopts β-sheet secondary structure and forms amyloid fibrils as that which occurs with Aβ-protein deposition [24]. Therefore, this study stems from the hypothesis that AChE could play a role in PrP aggregation.

Fluorescence microscopy analysis showed that the formation of coumarin-PrP 106–126 aggregates is extremely rapid since the MSA value already reached the peak value after 1 h

(983 ± 102 μm^2 after 1 h as compared to 1111 ± 137 μm^2 after 72 h, Fig. 1). These data are consistent with those previously reported in sedimentation experiments reporting that the soluble peptide fraction was already undetectable in the supernatant after 1 h of incubation [25]. Time-course experiments carried out in the presence of AChE (2.5 μM) showed a significant and progressive increase of MSA, achieving higher values between 48 h and 72 h of incubation ($13{,}600 \pm 136$ and $13{,}943 \pm 502$ μm^2, respectively; $p < 0.001$; Figs. 1 and 3A). Remarkably, after 1 h of

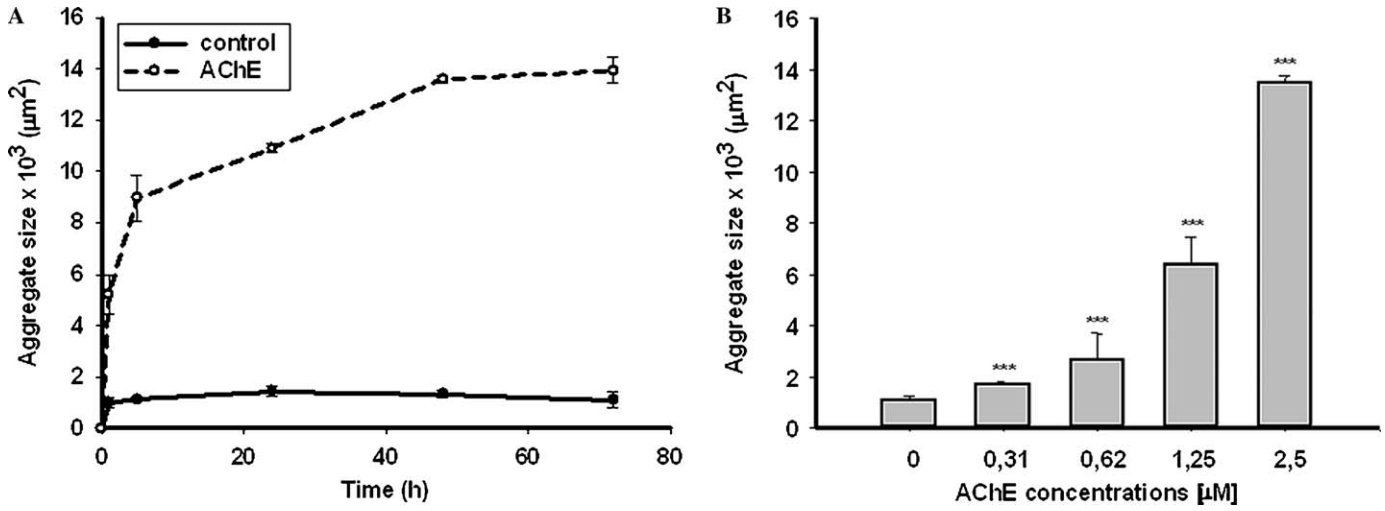

Fig. 1. (A) Time-course of MSA (maximum aggregate size) formation of coumarin-PrP 106–126 (1 mM) in the absence or in the presence of AChE (2.5 μM) in 100 mM Tris–HCl, pH 7.0, at room temperature. (B) MSA values of coumarin-PrP 106–126 (1 mM) incubated for 48 h with increasing AChE concentrations. Samples were analyzed by light fluorescence microscopy and the MSA was quantified by the Leica Qwin standard-image analysis program. Results are expressed as means ± SEM of the maximum size of aggregates (MSA; μm^2) of at least four experiments run in triplicate. ***$p < 0.001$ versus control group.

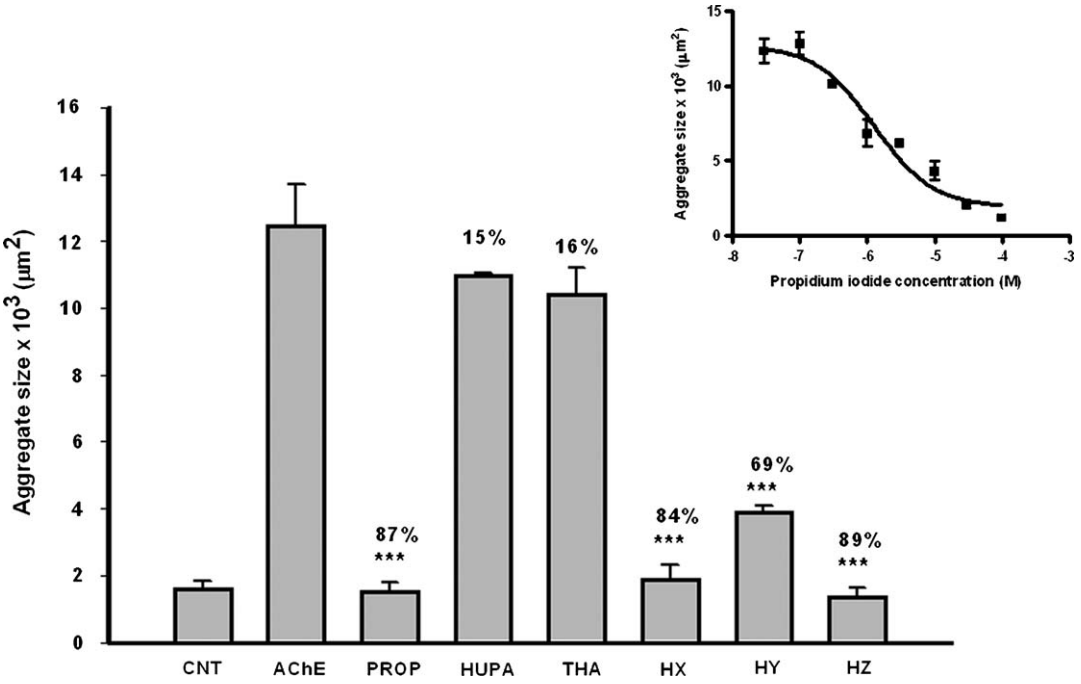

Fig. 2. Inhibition of AChE-induced aggregation of coumarin-PrP 106–126 by AChE inhibitors after 48 h of incubation assayed at a concentration of 100 μM: PROP (propidium iodide), HUPA (huperzine A), THA (tacrine), HX (huprine X), HY (huprine Y), and HZ (huprine Z). Values above bars represent the percentage of inhibition of MSA induced by AChEI. Inset represents concentration-response curve of propidium iodide in the presence of 2.5 μM AChE ($IC_{50} = 1.27 \pm 0.1$ μM) after 48 h of incubation. The IC_{50} (molar concentration of drug which produces the 50% of maximal effect) value was calculated by nonlinear regression analysis of experimental data using GraphPad Prism program (GraphPad Software Inc., Calinfornia). Results are expressed as means ± SEM of the maximum size of aggregates (MSA; μm^2) of at least 4 experiments run in triplicate. ***$p < 0{,}001$ versus AChE group.

incubation, MSA values ($5224 \pm 563\ \mu m^2$) were much higher than control samples devoid of AChE. The kinetics of aggregation of coumarin-PrP 106–126 was more pronounced and constant in time, as compared to Aβ, since Aβ attained the highest value of aggregation after 8 h of incubation [13,14]. In our experimental conditions, the highest aggregation was obtained between 48 and 72 h of incubation, and MSA values were approximately 12-fold higher than those of control samples. Moreover, a positive correlation between AChE concentration and coumarin-PrP 106–126 aggregation was also observed (Fig. 2) similar to previously described for Aβ [13,14].

Although there is no evident sequence or structural homology among the proteins involved in protein conformational disorders, there is accumulating evidence that the aggregates formed by misfolded proteins have the same final molecular structure [24]. Studies using shorter Aβ fragments have shown that the internal hydrophobic region between aminoacids 17 and 21 is the most important for the early steps of Aβ misfolding and aggregation, indicating that Aβ assembly is partially driven by hydrophobic interactions [26]. Similar studies on PrP conversion reaction have identified the 106–126 hydrophobic segment as relevant for protein aggregation [18]. The finding that hydrophobic sequences are critical for Aβ and PrP aggregation indicates that protein aggregation is driven by the exposure of hydrophobic residues to the surface of the misfolded protein [24].

The structural peripheral anionic motif of AChE involved in the binding with Aβ is a hydrophobic sequence exposed on the surface of the enzyme and it has been demonstrated that a synthetic 35-residue peptide corresponding to such sequence is incorporated into the growing Aβ fibrils by a hydrophobic interaction [27]. Aβ has a marked tendency to interact with hydrophobic environments and it has been reported that hydrophobic interactions may play a role in stabilizing the AChE-Aβ complex [13].

PrP 106–126 shows a conformational polymorphism in solution which supports the role of this fragment in the structural transition of the native to the abnormal form of PrP in response to changes in the local environmental conditions [19]. Molecular dynamic simulations carried out in different environments have shown an increased presence of helical structures in apolar solvents, in agreement with the results from circular dichroism spectroscopy. In water solution, β-sheet elements were observed between residues 108 and 112 and either residues 115–121 or 121–126. An α-transition was observed under neutral conditions. In dimethyl sulfoxide the peptide adopted an extended conformation, in agreement with nuclear magnetic resonance experiments [28]. It can therefore be postulated that the remarkable increase of

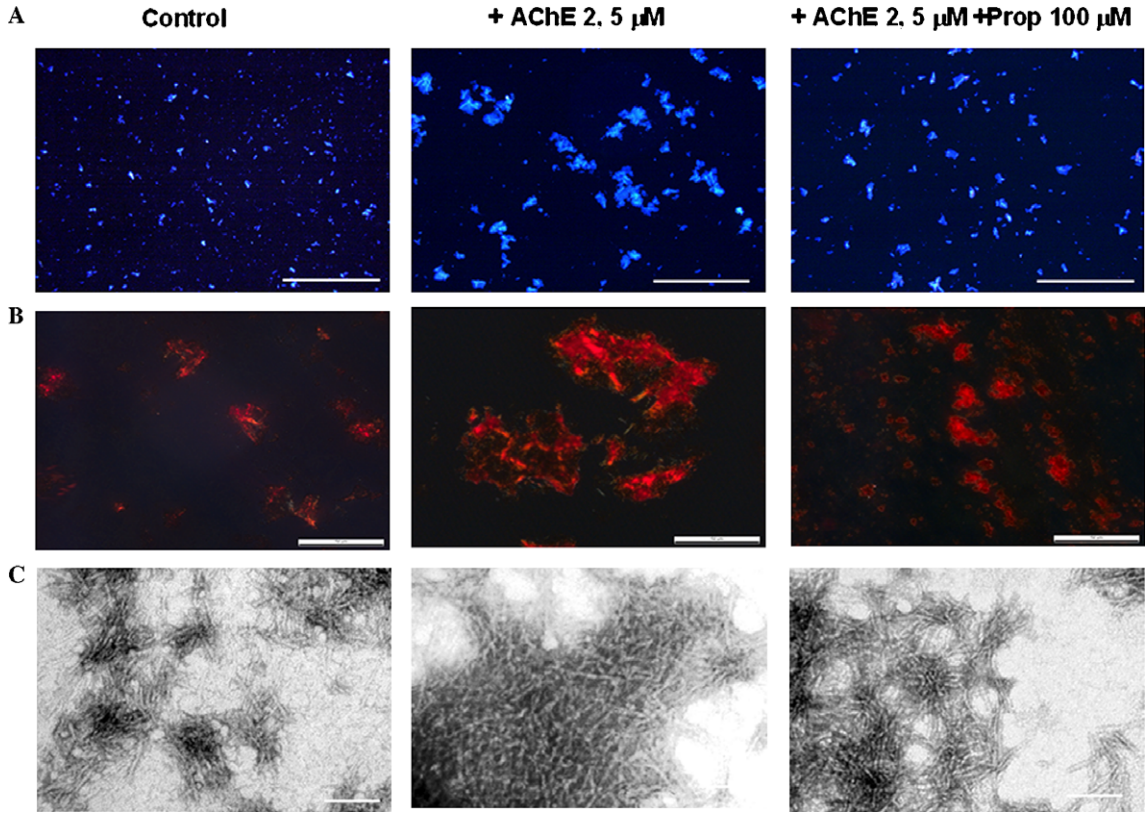

Fig. 3. (A) Fluorescence micrographs of aggregates generated in vitro by coumarin-PrP 106–126 (1 mM): (1) controls, (2) AChE 2.5 μM, and (3) AChE and propidium iodide (100 μM) following 48 h of incubation. Magnification 10×. Scale bar 100 μm. (B) Congo Red staining of PrP 106–126 (1 mM) aggregates analyzed by polarized light microscopy: (1) controls, (2) AChE 2.5 μM, and (3) AChE and propidium iodide (100 μM) following 48 h of incubation. Magnification 40×. Scale bar 50 μm. (C) Electron micrographs of aggregates generated in vitro by PrP 106–126 (1 mM), as revealed by negative staining of peptide suspensions: (1) controls, (2) AChE 2.5 μM, and (3) AChE and propidium iodide (100 μM) following 48 h of incubation. Magnification 70,000×. Scale bar 100 nm.

PrP 106–126 aggregation by AChE is mediated by the interaction with the structural peripheral anionic motif of the enzyme.

The nature of aggregates generated by PrP 106–126 in the absence and in the presence of AChE was examined under polarized light and electronic microscopy. As reported in Fig. 3B, macromolecular assemblies of PrP 106–126 and AChE-PrP 106–126 showed the tinctorial and optical properties of in situ amyloid, i.e., birefringence under polarized light after Congo Red staining. Birefringent properties of aggregates were more evident when AChE was present owing to the remarkable increase in the size of aggregates. The amyloid structure of the aggregates was also confirmed by electron microscope analysis. In the absence and in the presence of AChE, negative-stained PrP 106–126 assemblies showed that aggregates are composed of 4–8 nm thick unbranched fibrils, and no major morphological differences were detected among them (Fig. 3C). The amount of amyloid fibers found on the electron microscope grids was higher in the presence of the enzyme.

Propidium iodide is the most specific inhibitor interacting at the peripheral site of AChE, [15] and it has been extensively demonstrated that it inhibits the AChE-induced Aβ aggregation [12–14]. Accordingly, when coumarin-PrP 106–126 and AChE were co-incubated with propidium iodide, an IC_{50} of 1.27 ± 0.1 μM was obtained and an inhibition of 87% of MSA was observed at 100 μM (Figs. 2 and 3A). This value is almost identical to that previously described for AChE-induced Aβ aggregation under similar experimental conditions [14]. Therefore, the fact that propidium iodide, a specific inhibitor binding to the peripheral site of the enzyme, was able to revert the effect of AChE on PrP 106–126 aggregation in a concentration-dependent manner, strongly suggests that AChE induces PrP 106–126 and Aβ aggregation through the same site.

Using the same experimental conditions tacrine and huperzine A were devoid of any significant anti-aggregating effect, with a percentage of inhibition very similar to that previously reported for AChE-induced Aβ aggregation in the case of tacrine [14]. Although it has been recently demonstrated that some tacrine-based heterodimers can inhibit the AChE-induced Aβ aggregation [29], it is known that both tacrine and huperzine A show a high affinity for the catalytic site of AChE but not to the peripheral anionic one [30,31]. Huprines have recently emerged as a new class of potent and selective acetylcholinesterase inhibitors, which were designed from tacrine and huperzine A through a conjunctive approach [32–34]. Although huprines bind preferentially to the acylation site of AChE, experimental data and molecular modeling studies have demonstrated that the huprine X binding geometry and its molecular volume result in a significant decrease in the affinity of ligands to the peripheral site of the enzyme [34]. Huprines included in the present study clearly inhibited the AChE-induced PrP 106–126 aggregation in a percentage of inhibition near to that obtained in the presence of propidium (100 μM), especially huprine X and huprine Z (84% and 89%, respectively; Fig. 2), while huprine Y induced an anti-aggregating effect of 63%.

In conclusion, we report here, for the first time, that AChE induces a remarkable aggregation of PrP 106–126 with a mechanism similar to that described for Aβ. Noteworthy, the analysis carried out by polarized light and electron microscopy confirmed the amyloid nature of peptide assemblies. The inhibition of this effect by propidium iodide indicates the involvement of the AChE peripheral anionic site, suggesting that the pro-aggregating effect of this enzyme could play a more general role in the process of amyloid formation that is not confined to Aβ. In addition, our data unveil the relevance of some AChE inhibitors as potential anti-prion drugs.

Acknowledgments

We acknowledge the technical assistance of the Servei de Diagnostic de Patología Veterinaria and of the Servei de Microscopia from the Universitat Autonoma de Barcelona. This work was supported by DGICYT (SAF2002-00049) and CIRIT (2001SGR00216), the European Union within the frame of Neuroprion and Heteroprion networks (Contract No: FOOD-CT-2004-506579), Negri-Weizmann Foundation (2006), the Italian Ministry of University and Research (FIRB Protocol RBNE03PX83, 2005), and Fondazione Cariplo (Project Genoproteomics of Age Related Disorders, 2006).

References

[1] J. Tateishi, T. Kitamoto, H. Hashiguchi, H. Shii, Gerstmann–Straussler–Scheinker disease: immunohistological and experimental studies, Ann. Neurol. 24 (1988) 35–40.
[2] K.M. Pan, M. Baldwin, J. Nguyen, M. Gasset, A. Serban, D. Groth, I. Mehlhorn, Z. Huang, R.J. Fletterick, F.E. Cohen, et al., Conversion of alpha-helices into beta-sheets features in the formation of the scrapie prion proteins, Proc. Natl. Acad. Sci. USA 90 (1993) 10962–10966.
[3] S.B. Prusiner, Molecular biology of prion diseases, Science 252 (1991) 1515–1522.
[4] J.A. Hainfellner, J. Wanschitz, K. Jellinger, P.P. Liberski, F. Gullotta, H. Budka, Coexistence of Alzheimer-type neuropathology in Creutzfeldt–Jakob disease, Acta Neuropathol. 96 (1998) 116–122.
[5] K. Schwarze-Eicker, K. Keyvani, N. Gortz, D. Westaway, N. Sachser, W. Paulus, Prion protein (PrP(c)) promotes beta-amyloid plaque formation, Neurobiol. Aging 26 (2005) 1177–1182.
[6] R.A. Armstrong, P.L. Lantos, N.J. Cairns, Spatial correlations between the vacuolation, prion protein deposits, and surviving neurons in the cerebral cortex in sporadic Creutzfeldt–Jakob disease, Neuropathology 21 (2001) 266–271.
[7] G.G. Kovacs, H. Budka, Aging, the brain and human prion disease, Exp. Gerontol. 37 (2002) 603–606.
[8] M. Miyazono, T. Kitamoto, T. Iwaki, J. Tateishi, Colocalization of prion protein and beta protein in the same amyloid plaques in patients with Gerstmann-Straussler syndrome, Acta Neuropathol. 83 (1992) 333–339.
[9] C. Gohel, V. Grigoriev, F. Escaig-Haye, C.I. Lasmezas, J.P. Deslys, J. Langeveld, M. Akaaboune, D. Hantai, J.G. Fournier, Ultrastructural

localization of cellular prion protein (PrPc) at the neuromuscular junction, J. Neurosci. Res. 55 (1999) 261–267.
[10] S. Petrakis, I. Paspaltsis, J. Lindstrom, T. Sklaviadis, PrPC coimmunoprecipitates with nicotinic acetylcholine receptor B4 subunit in normal human brain. First international congress of neuroprion (France) (2004).
[11] D.A. Harris, P. Lele, W.D. Snider, Localization of the mRNA for a chicken prion protein by in situ hybridization, Proc. Natl. Acad. Sci. USA 90 (1993) 4309–4313.
[12] N.C. Inestrosa, A. Alvarez, C.A. Perez, R.D. Moreno, M. Vicente, C. Linker, O.I. Casanueva, C. Soto, J. Garrido, Acetylcholinesterase accelerates assembly of amyloid-beta-peptides into Alzheimer's fibrils: possible role of the peripheral site of the enzyme, Neuron 16 (1996) 881–891.
[13] A. Alvarez, C. Opazo, R. Alarcon, J. Garrido, N.C. Inestrosa, Acetylcholinesterase promotes the aggregation of amyloid-beta-peptide fragments by forming a complex with the growing fibrils, J. Mol. Biol. 272 (1997) 348–361.
[14] M. Bartolini, C. Bertucci, V. Cavrini, V. Andrisano, beta-Amyloid aggregation induced by human acetylcholinesterase: inhibition studies, Biochem. Pharmacol. 65 (2003) 407–416.
[15] T. Szegletes, W.D. Mallender, P.J. Thomas, T.L. Rosenberry, Substrate binding to the peripheral site of acetylcholinesterase initiates enzymatic catalysis. Substrate inhibition arises as a secondary effect, Biochemistry 38 (1999) 122–133.
[16] E.O. Campos, A. Alvarez, N.C. Inestrosa, Brain acetylcholinesterase promotes amyloid-beta-peptide aggregation but does not hydrolyze amyloid precursor protein peptides, Neurochem. Res. 23 (1998) 135–140.
[17] C. Selvaggini, L. De Gioia, L. Cantu, E. Ghibaudi, L. Diomede, F. Passerini, G. Forloni, O. Bugiani, F. Tagliavini, M. Salmona, Molecular characteristics of a protease-resistant, amyloidogenic and neurotoxic peptide homologous to residues 106–126 of the prion protein, Biochem. Biophys. Res. Commun. 194 (1993) 1380–1386.
[18] F. Tagliavini, F. Prelli, L. Verga, G. Giaccone, R. Sarma, P. Gorevic, B. Ghetti, F. Passerini, E. Ghibaudi, G. Forloni, M. Salmona, O. Bugiai, B. Frangione, Synthetic peptides homologous to prion protein residues 106–147 form amyloid-like fibrils in vitro, Proc. Natl. Acad. Sci. USA 90 (1993) 9678–9682.
[19] L. De Gioia, C. Selvaggini, E. Ghibaudi, L. Diomede, O. Bugiani, G. Forloni, F. Tagliavini, M. Salmona, Conformational polymorphism of the amyloidogenic and neurotoxic peptide homologous to residues 106–126 of the prion protein, J. Biol. Chem. 269 (1994) 7859–7862.
[20] G. Forloni, N. Angeretti, R. Chiesa, E. Monzani, M. Salmona, O. Bugiani, F. Tagliavini, Neurotoxicity of a prion protein fragment, Nature 362 (1993) 543–546.
[21] S. Thellung, T. Florio, A. Corsaro, S. Arena, M. Merlino, M. Salmona, F. Tagliavini, O. Bugiani, G. Forloni, G. Schettini, Intracellular mechanisms mediating the neuronal death and astrogliosis induced by the prion protein fragment 106–126, Int. J. Dev. Neurosci. 18 (2000) 481–492.
[22] S. Thellung, T. Florio, V. Villa, A. Corsaro, S. Arena, C. Amico, M. Robello, M. Salmona, G. Forloni, O. Bugiani, F. Tagliavini, G. Schettini, Apoptotic cell death and impairment of L-type voltage-sensitive calcium channel activity in rat cerebellar granule cells treated with the prion protein fragment 106–126, Neurobiol. Dis. 7 (2000) 299–309.
[23] F.B. Hafiz, D.R. Brown, A model for the mechanism of astrogliosis in prion disease, Mol. Cell Neurosci. 16 (2000) 221–232.
[24] C. Soto, Unfolding the role of protein misfolding in neurodegenerative diseases, Nat. Rev. Neurosci. 4 (2003) 40–60.
[25] M. Salmona, P. Malesani, L. De Gioia, S. Gorla, M. Bruschi, A. Molinari, V.F. Della, B. Pedrotti, M.A. Marrari, T. Awan, O. Bugiani, G. Forloni, F. Tagliavini, Molecular determinants of the physicochemical properties of a critical prion protein region comprising residues 106–126, Biochem. J. 342 (1999) 207–214.
[26] C. Hilbich, B. Kisters-Woike, J. Reed, C.L. Masters, K. Beyreuther, Substitutions of hydrophobic amino acids reduce the amyloidogenicity of Alzheimer's disease beta A4 peptides, J. Mol. Biol. 228 (1992) 460–473.
[27] G.V. De Ferrari, M.A. Canales, I. Shin, L.M. Weiner, I. Silman, N.C. Inestrosa, A structural motif of acetylcholinesterase that promotes amyloid beta-peptide fibril formation, Biochemistry 40 (2001) 10447–10457.
[28] A. Villa, A.E. Mark, G.A. Saracino, U. Cosentino, D. Pitea, G. Moro, M. Salmona, Conformational polymorphism of the PrP 106–126 peptide in different environments: a molecular dynamics study, J. Phys. Chem. B Condens. Matter Mater. Surf. Interfaces. Biophys. 110 (2006) 1423–1428.
[29] P. Munoz-Ruiz, L. Rubio, E. Garcia-Palomero, I. Dorronsoro, M. Monte-Millan, R. Valenzuela, P. Usan, C. de Austria, M. Bartolini, V. Andrisano, A. Bidon-Chanal, M. Orozco, F.J. Luque, M. Medina, A. Martinez, Design, synthesis, and biological evaluation of dual binding site acetylcholinesterase inhibitors: new disease-modifying agents for Alzheimer's disease, J. Med. Chem. 48 (2005) 7223–7233.
[30] H.A. Berman, K. Leonard, Interaction of tetrahydroaminoacridine with acetylcholinesterase and butyrylcholinesterase, Mol. Pharmacol. 41 (1992) 412–418.
[31] N. Ariel, A. Ordentlich, D. Barak, T. Bino, B. Velan, A. Shafferman, The 'aromatic patch' of three proximal residues in the human acetylcholinesterase active centre allows for versatile interaction modes with inhibitors, Biochem. J. 335 (1998) 95–102.
[32] A. Badia, J.E. Baños, P. Camps, J. Contreras, D.M. Görbigb, D. Muñoz-Torrerob, M. Simón, N.M. Vivas, Synthesis and evaluation of tacrine-huperzine A hybrids as acetylcolinesterase inhibitors of potential interest for the treatment of Alzheimer's disease, Bioorg. Med. Chem. 6 (1998) 427–440.
[33] P. Camps, R. El Achab, D.M. Gorbic, J. Morral, D. Muñoz-Torrero, A. Badia, J.E. Baños, N.M. Vivas, X. Barril, M. Orozco, F.J. Luque, Synthesis, in vitro pharmacology, and molecular modeling of very potent tacrine-huperzine A hybrids as acetylcholinesterase inhibitors of potential interest for the treatment of Alzheimer's disease, J. Med. Chem. 42 (1999) 3227–3242.
[34] P. Camps, B. Cusack, W.D. Mallender, R.E. El Achab, J. Morral, D. Munoz-Torrero, T.L. Rosenberry, Huprine X is a novel high-affinity inhibitor of acetylcholinesterase that is of interest for treatment of Alzheimer's disease, Mol. Pharmacol. 57 (2000) 409–417.